Photoacoustic and X-ray photoelectron spectroscopic studies in reduced lead zirconate titanate ceramics

N. R. RAJOPADHYE, S. V. BHORASKAR*
Department of Physics, University of Poona, Pune 411 007, India

S. BADRINARAYAN, A. P. B. SINHA
National Chemical Laboratory, Pune 411 008, India

Lead zirconate titanate (PZT) is known to become a semiconductor after reduction in a hydrogen atmosphere. An attempt is made here to characterize the reduced, as well as the unreduced, PZT system with the help of photoacoustic (PA) spectroscopy and X-ray photoelectron spectroscopy (XPS) and to obtain useful information regarding its electronic behaviour.

The band gap of the unreduced PZT is estimated to be 3.56 eV from PA spectra which is observed to remain unaffected after doping with lanthanum, niobium and strontium. XPS results indicate the presence of metallic lead in PZT after hydrogen reduction whereas other elements remain unaffected. This becomes responsible for the change in its conductivity and also for the increased absorption in the visible range which is reflected in the PA spectra. The electronic structure based on PA spectra is also presented for the reduced and unreduced PZT systems.

1. Introduction

Multioxide systems are a versatile class of materials for several solid state devices and therefore knowledge of their electronic structure is important. This paper presents the applicability of photoacoustic spectroscopy for evolving useful information about one of the mixed oxide systems namely lead zirconate titanate (PZT). The results have been supplemented by the X-ray photoelectron spectroscopy (XPS) data.

Recently semiconducting ceramics have been identified as useful electronic materials [1–3] for scientific and technological applications. It has been observed that PZT also becomes semiconducting after reducing it in a hydrogen atmosphere. Since the resistivity can be controlled by varying the parameters involved in the reduction treatment, reduced PZT poses potential as a semiconducting ceramic. However, the electronic behaviour of PZT is not fully explored so far. An attempt has, therefore, been made to investigate the chemical reaction responsible for the electrical conduction in the reduced PZT sample. The valence changes in the reduced sample, which play a major role in the conduction mechanism, were identified by using X-ray photoelectron spectroscopy. The electronic structure based on photoacoustic spectroscopy (PA) spectra is also presented for the first time for reduced and unreduced PZT systems.

2. Experimental details

The conventional powder method was adopted for the preparation of PZT. Samples were prepared in the shape of circular pellets (15 mm diameter) having a thickness of 1.5 mm. Reagent grade oxides of PbO, ZrO_2, TiO_2 and the appropriate oxide of the dopant elements were mixed in suitable proportions by weight to obtain $Pb_{0.95}D_{0.05}(Zr_{0.53}Ti_{0.47})O_3$ where D indicates the dopant. The material was calcined at 1020 K for 4 to 6 hours. The mixture was pressed in stainless steel moulds in samll hydraulic press with compacting pressure of 6 kg m^{-2} to form pellets of the required size.

After compression, the pellets were sintered in air at about 1563–1573 K for 90 min. Loss of volatile PbO was prevented by adding an excess amount of PbO during preparation of the batch. The density of the final product was $7.6 \times 10^3 \text{ kg m}^{-3}$ which was in good agreement with the theoretically calculated density [4].

The reduction of PZT was carried out in a hydrogen zone furnace at 873 K for 10 min. The parameters were optimized in order to obtain the required resistivity of $10^7 \Omega \text{ cm}$.

XPS measurements were recorded on ESCA-3, MK-II electron spectrometer, using AlK X-ray (1486.6 eV) source at a pressure less than 10^{-9} torr. Spectra were then analysed using least square fitting for the Gaussian function. The EDT model OAS400 was used for studying the photoacoustic absorption.

3. Results and discussion
3.1. Electrical conductivity results

The sintered PZT samples were pale yellow in colour and changed to black after reduction. The sheet resistivity decreased from 10^{12}–$10^{13} \Omega \text{ cm}$ for the unreduced samples to 10^6–$10^7 \Omega \text{ cm}$ for the reduced

*Author to whom correspondence should be addressed.

TABLE I Lead to lead oxide ratio observed from lead 4f XPS spectra (Fig. 1) in unreduced and reduced Nb-PZT at different depths

Etching time minutes	Unreduced	Reduced
	Pb : PbO	Pb : PbO
0	0 : 1.0	0 : 1.0
5	0 : 1.0	1.045 : 1.0
20	0 : 1.0	1.58 : 1.0
65	0 : 1.0	2.00 : 1.0

TABLE II TiO to TiO_2 ratio observed from titanium 2p XPS spectra (Fig. 2) in unreduced reduced Nb-PZT at different depths

Etching time minutes	Unreduced	Reduced
	$TiO : TiO_2$	$TiO : TiO_2$
0	0 : 1.0	0 : 1.0
5	0.22 : 1.0	0.29 : 1.0
20	0.27 : 1.0	0.23 : 1.0
65	0.27 : 1.0	0.25 : 1.0

samples. This reaction was found to be reversible in the sense that the sample returned to its original colour and the resistivity regained its virgin value after heating in the atmosphere at 473 K for a few minutes. Moreover from the investigation of the colour variation in a section cut normal to the plane it was observed that the process of reduction has affected only a limited region near the sample surface; which was found to vary between 15 and $20\,\mu m$ from the optical microscopic measurements.

In the present experiment the increase in conductivity after the reduction may be expected to be due to the migration of oxygen from the bulk as well as loss from the surface. Therefore, in a reduced system the valence change may, in principle, occur with either lead, zirconium, titanium or a combination of them all. However, the exact site of valence change in such a complex system (PZT) has not been investigated so far. In this case XPS analysis is expected to clarify the situation in reaction products in view of its analytical capability.

4. XPS results

The XPS spectra are presented for one of the doped species for an Nb-PZT, on uncleaned surface and after suitable intervals while etching the sample with argon

ion bombardment for a total duration of about an hour. The ion beam of 5 keV energy was focused on a $1\,cm^2$ area of the sample with the beam current of $40-50\,\mu A$.

Many oxides, on argon ion bombardment, are found [5-7] to be reduced to lower oxides. Hence it is essential to take this into account while analysing the depth profiled data obtained through ion bombardment. It is for this reason that the depth profiled spectra of an unreduced sample are presented for comparison. The relative intensities of few of the species obtained after Gaussian fitting are shown in Tables I and II.

Fig. 1 shows the XPS of lead $4f_{7/2}-4f_{5/2}$ levels for unreduced and reduced samples. The doublet at the binding energy of 139 eV and 143.8 eV observed on the surface of unreduced PZT is assigned to PbO. Even after prolonged ion etching neither change in the line shape of the lead 4f level nor any binding energy shift was observed, indicating that ion bombardment has no effect on PbO. On the contrary the reduced PZT sample showed the presence of metallic lead (Pb^0) (137.0 eV and 141.8 eV) along with its oxide. It is reasonable, therefore, to assume that the presence of Pb^0 in the reduced sample is only due to hydrogen reduction. However contrary to the expectation, the
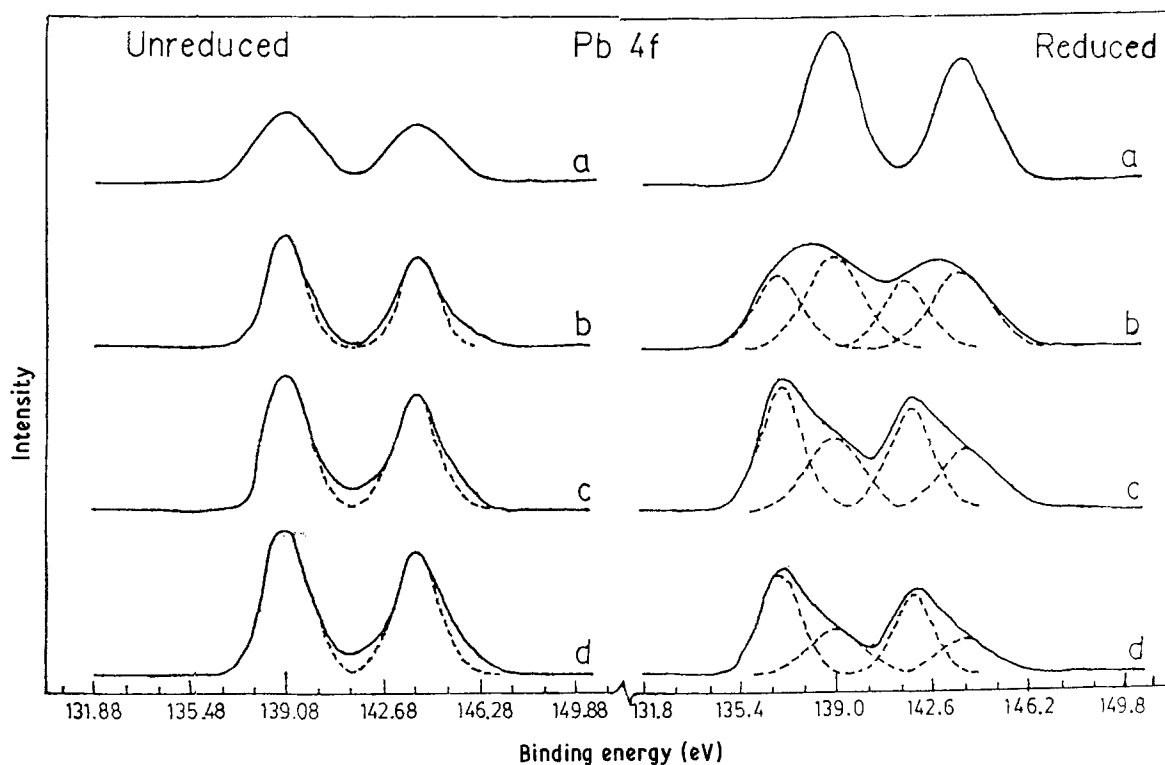

Figure 1 XPS spectra of lead $4f_{7/2}$ and lead $4f_{5/2}$ of unreduced and reduced Nb-PZT after successive etching with argon ion bombardment. (a) Surface (b) After 5 min etching (c) After 20 min etching (d) After 65 min etching. The dotted curves show the resolved peaks.
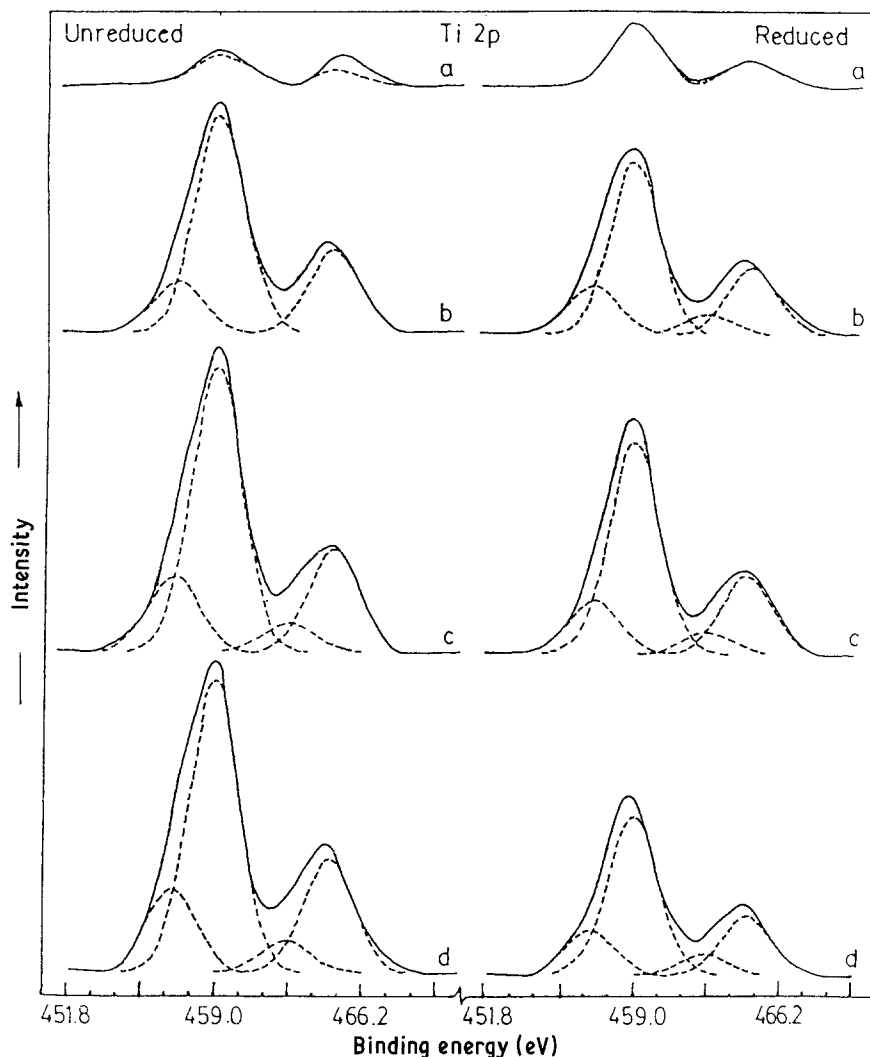
Figure 2 Titanium $2p_{3/2}$ and $2p_{1/2}$ XPS spectra in unreduced and reduced Nb-PZT. The notations are the same as in Fig. 1. This indicates that observed reduction in reduced sample is because of the ion bombardment.

Pb^0 concentration is found to decrease near the surface (Table I). This presumably is due to reoxidation during cooling in nitrogen ambiant.

XPS spectra of the titanium 2p level are presented in Fig. 2. From the resolved peaks it is seen that lower oxidation states of titanium are produced in both unreduced and reduced samples. Here the peaks at binding energies of 457.3 eV and 463.1 eV are assigned [8] to TiO and 459.0 and 464.8 eV to TiO_2. However the quantitative analysis shown in Table II reveals that the extent of reduction does not differ appreciably in both samples and thus leads to the conclusion that TiO_2 in the reduced sample has not been affected by hydrogen reduction. This is surprising because titanium is popularly known to be reduced by hydrogen annealing from Ti^{4+} to Ti^{3+}. Most probably this is due to the presence of lead and its higher sensitivity for reduction at relatively lower temperatures.

The spectra were also recorded for zirconium 3d lines which showed that neither ion bombardment nor hydrogen has caused any noticeable reduction in this oxide. The spectra of niobium 3d indicated the presence of NbO, NbO_2 and Nb_2O_5 in both samples but to the same extent. This again proved that the effect of valence change in niobium was due to ion bombardment and not hydrogen reduction.

From the above measurements it is seen that reduced PZT has a specific nature showing a trend of loss of oxygen and thus producing a lower oxidation state in lead.
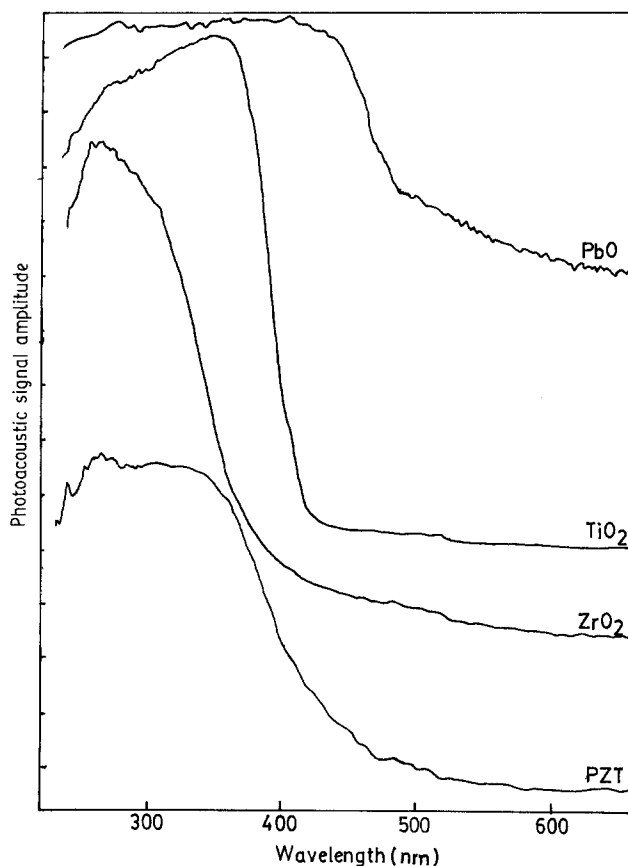

Figure 3 Photoacoustic spectra of PbO, ZrO_2, TiO_2 and sintered PZT pellet. The PA spectrum of PZT retains the spectral features of constituent oxides.
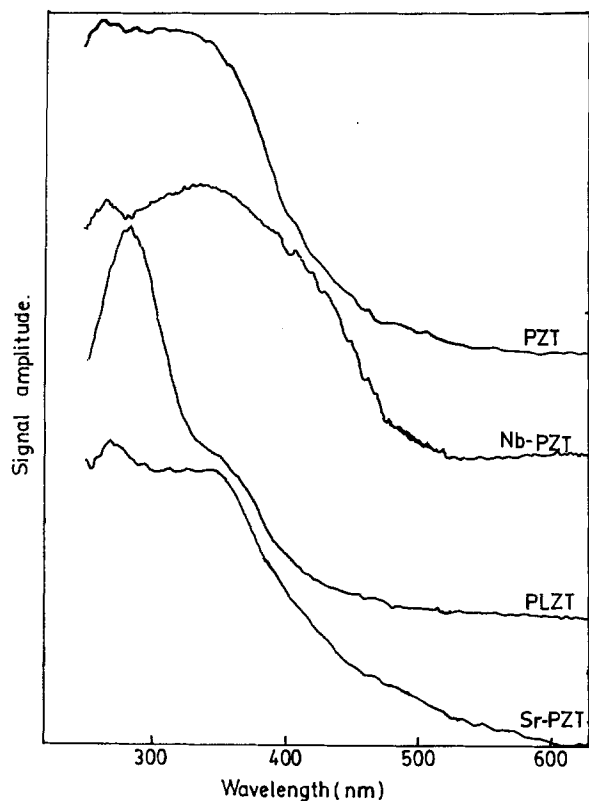
Figure 4 PA spectra of undoped PZT, PLZT, Nb-PZT and Sr-PZT. This shows that the bandgap has remained same after doping.

5. Photoacoustic spectroscopic studies

Fig. 3 shows the PA spectra of reagent grade powders of PbO, ZrO_2 and TiO_2 and sintered pellets of PZT. The optical absorption edges for PbO, ZrO_2 and TiO_2 are thus obtained at 430 nm, 310 nm and 370 nm respectively (as measured by the position of the knee). The absorption due to PbO in the visible range predominantly decides the onset of absorption in the sintered PZT pellets at around 500 nm and causes the yellow colour of the sample. The bandgap of PZT is estimated to be 3.56 eV (350 nm) which closely matches that reported by Krupanidhi et al. [9], determined from the optical absorption measurements for the sputtered films of PZT.

It is also seen from these spectra that strong peaks arise at 360 nm for TiO_2 and at 265 nm for ZrO_2 whereas no such peak is observed for PbO. These peaks suggest the presence of strong density of states (DOS) in the conduction band of the corresponding oxide. These are also reflected in the PA spectrum of the sintered PZT pellet. In effect one can say that optical absorption in PZT has been reflected by the combined effect of all three oxides.

Fig. 4 shows the PA spectra of undoped and doped PZT ceramics. It is interesting to see that the absorption edge remains at the same position in all the doped samples indicating that the bandgap in PZT has not changed due to the doping.

The PA spectra of reduced PZT, PLZT, Nb-PZT and Sr-PZT are shown in Fig. 5. The prominent effect of reduction on the absorption spectrum is seen in the range of 350 nm to 700 nm, where the overall absorption has increased. Due to this increased absorption the band edge has disappeared whereas the peak at
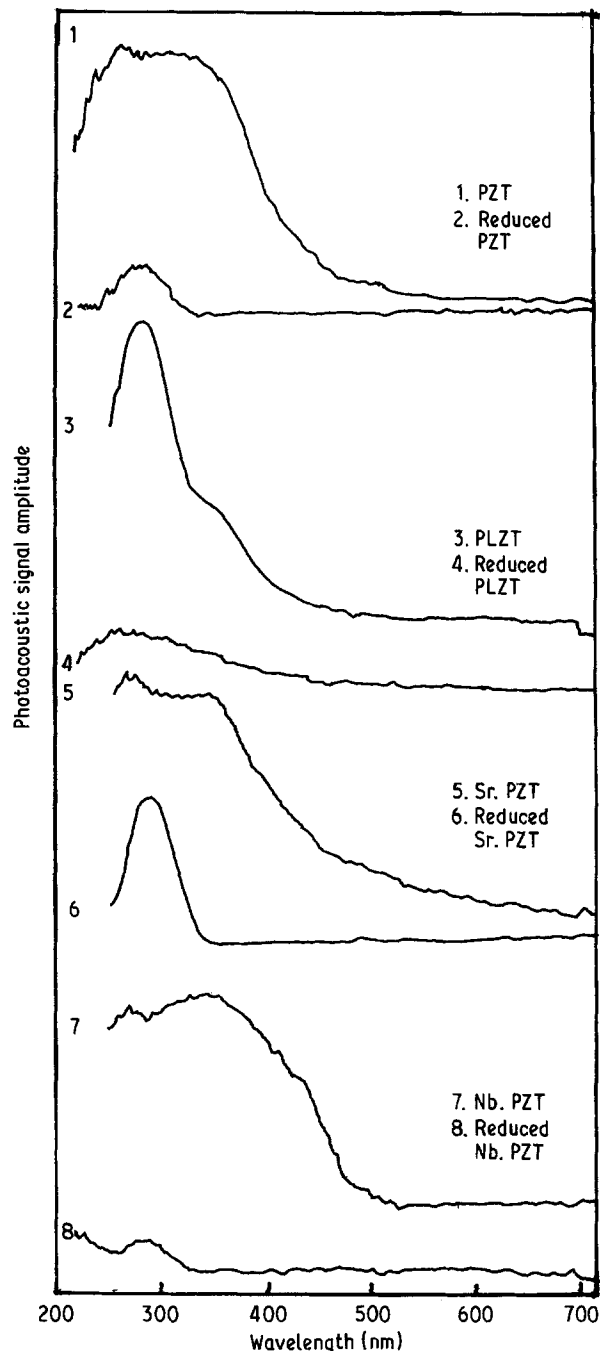

Figure 5 PA spectra of unreduced and reduced sample PZT, PLZT, Nb-PZT and Sr-PZT. The typical absorption edge has disappeared in each reduced sample.

280 nm has remained unaffected. The increased absorption indicates the large number of defect states produced due to the non-stoichiometry in reduced sample.

From the XPS results it is clear that PbO reduces to metallic lead. Experiments were performed, therefore, to study the role of metallic lead in affecting the PA spectra. Photoacoustic absorption was studied for PbO powder which was individually reduced for different time intervals (Fig. 6). This clearly indicates that the effect of metallic lead is only to increase the overall absorption. The other two oxides ZrO_2 and TiO_2 were also reduced for different temperatures and time intervals, however no change was observed in their PA spectra. This suggests that the peak at 280 nm can be correlated to the unaffected constituents in the reduced sample, namely ZrO_2 and TiO_2.
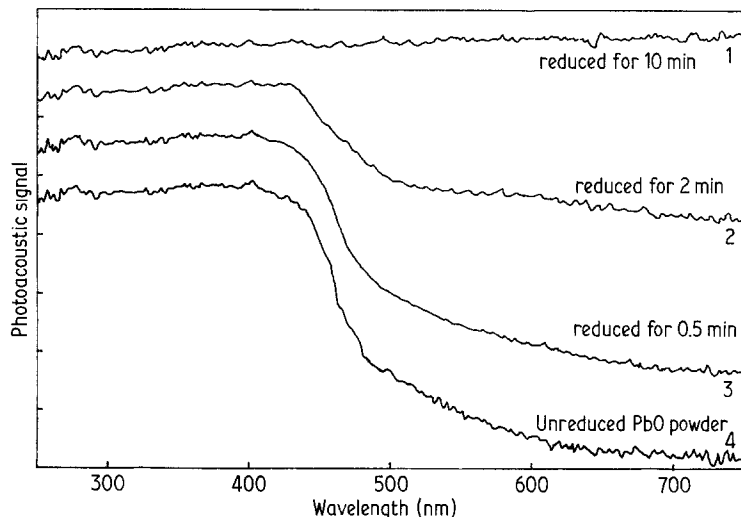
Figure 6 PA spectra of PbO powder, individually reduce to various extents. Curves 1, 2, and 3 corresponds to the reduction time duration of 10 min, 2 min and 0.5 min at 600° C. Curve 4 is PA spectrum of original powder. This indicates, that the role of dissociated metallic lead is only to increase the absorption.

Using the energy level values for free atoms one can obtain the approximate positions and sequence of the different energy levels. It is clear that the topmost filled band in PZT corresponds to the oxygen 2p energy level. The optical absorption edge observed in the PZT and reduced PZT at 350 nm can then be attributed to transition from this oxygen 2p filled band to the lowest lying empty level. The lowest lying empty levels are lead 6s, zirconium 4d and titanium 3d. These are very close in energy values and it is reasonable to presume that these empty levels overlap in the conduction band. This presumption is supported by the fact that the relative positions of most of the atomic energy levels of lead, zirconium and titanium have remained unchanged, as one goes from free atoms to compound PZT, as seen from the XPS data. On the basis of this presumption one can draw an energy level diagram, for the topmost levels, which is shown in Fig. 7a and b for unreduced and reduced PZT respectively. The topmost occupied level is that of oxygen 2p and the lowest empty band consists of lead 6s, zirconium 4d and titanium 3d. The d levels being more narrow, one expects a peak in the density of states (DOS) as shown in Fig. 7 which is reflected in the PA spectra. The peak at 280 nm (4.4 eV) can be correlated to the transition from oxygen 2p to the set of dense energy levels of titanium 3d/zirconium 4d (Fig. 7). Similarly, the

absorption edge at 350 nm (3.56 eV) is due to the transition from the top of oxygen 2p valence band to the bottom of conduction band. As discussed earlier the continuous absorption in the visible range observed in reduced PZT sample is due to free metallic lead. Metallic lead presumably has a broader conduction band extending in the energy region corresponding to the energy gap in the PZT samples. This leads to the increased absorption in the visible range and thereby disappearance of the optical absorption edge.

The spectra were also recorded at different modulating frequencies to obtain the depth profile of the reduced samples. This is shown in Fig. 8 for Sr-PZT. The spectra for other dopants follow the same trend. The amplitude of the absorption peak (280 nm) increases as one moves to the lower frequencies, as expected. The overall nature of the spectra remain the same for all modulation frequencies used in this measurement indicating that the effects of reduction are uniform over the depths studied in the reduced samples.

In conclusion we can say that

(1) Reduction of PZT ceramic produces free metallic lead. This is seen in XPS through the apprearance of Pb⁰ and in PA by the disappearance of the band gap caused by the continuous increased absorption in visible range.
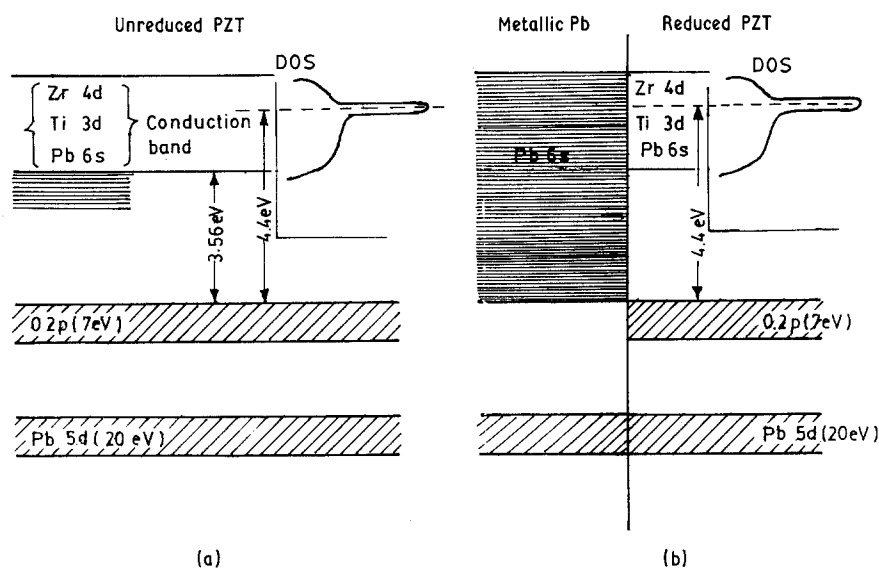

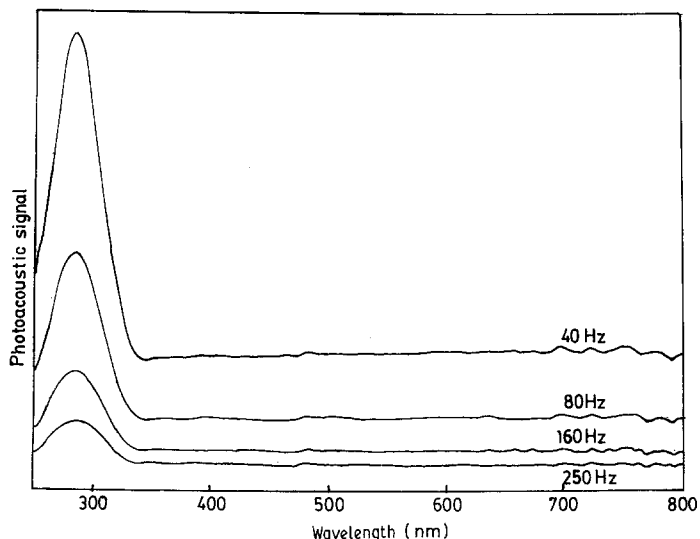*Figure 7* The energy level diagram based on PA spectra for unreduced and reduced PZT.

Figure 8 PA spectrum of reduced Sr-PZT for various modulation frequencies. The amplitude of PA signal increases for lower frequencies as expected.

(2) Nothing other than lead is affected by reduction. The metallic lead in the reduced sample is responsible for the change in the conductivity.

(3) The bandgap of PZT is evaluated to be 3.56 eV and is observed to remain unaltered even after doping.

(4) In PZT, the PA spectrum retains the spectral features of the individual oxides. The prominent peak at 280 nm (which is attributed to the transition from oxygen 2p to zirconium 4d/titanium 3d band) is characterized by its presence with strong intensity in unreduced as well as reduced PZT.

References

1. A. D. ANNIS and G. SIMPSON, *Infrared Phys.* **14** (1974) 199.
2. H. J. SANDERS, C & EN, Special Report, 26 (1984). (American Chemical Society).
3. T. MASUOKA, *Rev. Sci. Instrum.* **48** (1977) 1234.
4. B. JAFFE, R. S. ROTH and S. MARZULLO, *J. Res. Nat. Bur. Sci.* **55** (1955) 239.
5. K. S. KIM and N. WINOGRAD, *Surface Sci.* **43** (1974) 625.
6. K. S. KIM, W. E. BAITINGER and N. WINOGRAD, *Surface Sci.* **55** (1976) 285.
7. S. THOMAS, *Surface Sci.* **55** (1976) 754.
8. C. N. R. RAO, D. D. SARMA, S. VASUDEVAN and M. S. HEDGE, *Proc. R. Soc.* **A367** (1979) 239.
9. S. B. KRUPANIDHI and D. EL. ASSAL, *J. Appl. Phys.* **54** (1983) 6601.